

# Histological Skin Changes After Treatment with 675 nm Laser

Giovanni Cannarozzo, MD,<sup>1</sup> Luigi Bennardo, MD,<sup>2</sup> Tiziano Zingoni, Bsc,<sup>1</sup> Laura Pieri, PhD,<sup>3</sup> Ester Del Duca, MD,<sup>2</sup> and Steven Paul Nisticò, MD, PhD<sup>2</sup>

## Abstract

**Objective:** To evaluate the histological effects of a new 675-nm laser device on the skin.

**Background:** Innovative technologies based on physical principles have been proposed in recent years to improve the treatment of aging skin. Laser technology is currently being studied for its potential in skin care treatments. A new 675-nm laser device is being used for the treatment of hyperpigmentation, scars, and various types of wrinkles.

**Methods:** A 42-year-old man underwent a 675-nm RedTouch<sup>®</sup> laser session for the treatment of aging signs on the neck. Two 2.5-mm biopsies were taken from the treated area and the adjacent area untreated with the laser, 45 days after the procedure. Comparison of the immunohistochemistry findings and assessment of the collagen and elastin fibers were performed by a board-certified dermatopathologist.

**Results:** Skin biopsies revealed histological changes that comprised proliferation of new collagen fibers in the treated area, when compared to that in the untreated areas.

**Conclusions:** Histological analysis suggests that the 675-nm laser has a potential role in stimulating collagen remodeling, with a significant increase in thin and new collagen fibers.

**Keywords:** 675 nm, laser, histology, collagen

## Introduction

INNOVATIVE TECHNOLOGIES BASED on physical principles have been recently proposed to improve the treatment of aging skin. Laser technology is currently being studied for its potential in skin care treatments. A new 675-nm fractional laser (RedTouch<sup>®</sup>, Deka Medical Lasers, Florence, Italy) has recently been proposed for the treatment of aging skin, scars, and pigmentary disorders such as melasma.<sup>1–3</sup> The lasers in this wavelength show a high affinity for collagen fibers and melanin<sup>4</sup> with minimal interaction with hemoglobin.

Thermal and subablative selective dermal damage was observed in the treated areas. Epidermal heat damage was avoided because of an integrated skin cooling system at 5°C. RedTouch laser has been proven to have clinical efficacy in the treatment of hyperpigmentation and scars.<sup>1–3</sup> In this case report, we performed a histological analysis of treated and untreated aged skin and compared differences in collagen production of these two samples.

## Materials and Methods

A 42-year-old man with a Fitzpatrick III skin phototype was treated with a single session of the RedTouch laser using standard settings (Table 1) for signs of aging on the neck. A conductive transparent gel was used in the procedure and two laser passes were performed in the predetermined area (Ultrasound transmission Gel G007 Eco by Fiab, Vicchio, Italy). No pretreatment procedure was required. Epidermal heat damage was avoided because of an integrated skin cooling system at 5°C that was used during the procedure and a nonsteroidal anti-inflammatory cream applied daily for 7 days.<sup>5</sup> Postoperative recommendations included the use of total block mineral sunscreens for the entire treatment and follow-up periods. Assessment of the improvement in wrinkles and skin aging was performed by a board-certified dermatopathologist. Photographic documentation was performed using multi-spectral analysis (Antera 3D technologies, Miravex, Dublin, Ireland).

<sup>1</sup>Unit of Lasers in Dermatology, Università Roma Tor Vergata, Rome, Italy.

<sup>2</sup>Unit of Dermatology, Department of Health Sciences, Magna Graecia University, Catanzaro, Italy.

<sup>3</sup>Department of Biology, University of Florence, Florence, Italy.

TABLE 1. DEVICE TECHNICAL SPECIFICATIONS

<i>Technical specifications</i>	<i>Available</i>	<i>Used in the case report</i>
Wavelength	675 nm	675 nm
Power	Up to 10 W	10 W
Scan area size	Up to 15 × 15 mm	15 × 15 mm
Scanning shapes	Point, line, triangle, ellipse, hexagon, square	Square and ellipse
Scan modes	Normal, interlaced, SmartTrack	SmartTrack
Dwell time	50–1000 ms	300–400 ms
Spacing	0–4 mm	1–1.5 mm
SmartStack	1–5	1
Integrated skin cooler	Down to 5°C	5°C

The patient presented with a nodular lesion of 0.5 cm outside the treated area. The lesion was clinically indicative of inflamed seborrheic keratosis, which was surgically removed for cosmetic reasons and recurrent inflammation. The lesion was surgically removed from the adjacent skin 45 days after the Redtouch laser treatment. The lesion was histologically classified as seborrheic keratosis (Fig. 1).

One extremity of the diamond-shaped surgical excision involved an area treated with the 675-nm RedTouch laser. We compared the histology of this area to that at the other end of the surgical excision that was not treated with the laser, to evaluate the differences in collagen rearrangement. The patient provided informed consent for all the procedures performed and permitted supplemental collagen analysis at the extremities of the lesion. Local ethics committee approval was obtained (Calabria Centro Ethical Committee reference number 373/2019). The patient was treated and underwent excision biopsy in the dermatology department of the “Tor Vergata” university hospital in Rome, Italy. Histological examination was performed in the pathology department of the “Tor Vergata” university hospital in Rome, Italy.

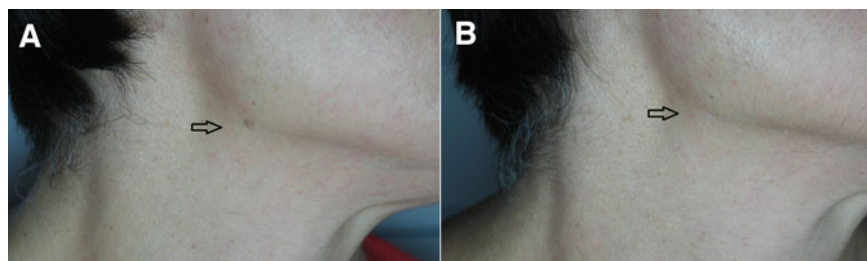
#### *Immunohistochemistry*

The specimens for histological analysis were fixed in 10% neutral formalin, after being dehydrated using a graded series of alcohol (or ethanol) solutions, cleared with Histoclear, and immersed in paraffin. Four-5- $\mu$ m thick sections were obtained and stained with hematoxylin and eosin (H&E) for evaluation using light microscopy. Specimens were evaluated with a Nikon Eclipse 80i light microscope (Nikon, Shinagawa, Tokyo, Japan). Collagen was stained using Van Gieson or picrosirius red, and elastin was stained using Weigert Van Gieson.<sup>6</sup> H&E staining was used to assess the epidermal thickness and inflammatory cell count. Dermal collagen fibers were studied using circularly polarized light and picrosirius red staining, which is capable of intensifying collagen birefringence.<sup>7–10</sup> The circularly polarized light method also allowed us to distinguish between

old collagen (red-orange) and newly formed collagen (green-yellow). Finally, images were exposed to binary segmentation (ImageJ; NIH, Bethesda, MD) of identical thresholds for the images to be compared. Digital morphometric analysis was performed. Photomicrographs were taken with a light microscope (Nikon) with suitable filters in the microscope tube and condenser stage. Images were recorded through a microscope digital photcamera (Nikon Digital Sight DS-U1; Nikon) connected to a personal computer containing the software Nis Elements D 3.2 (Nikon).

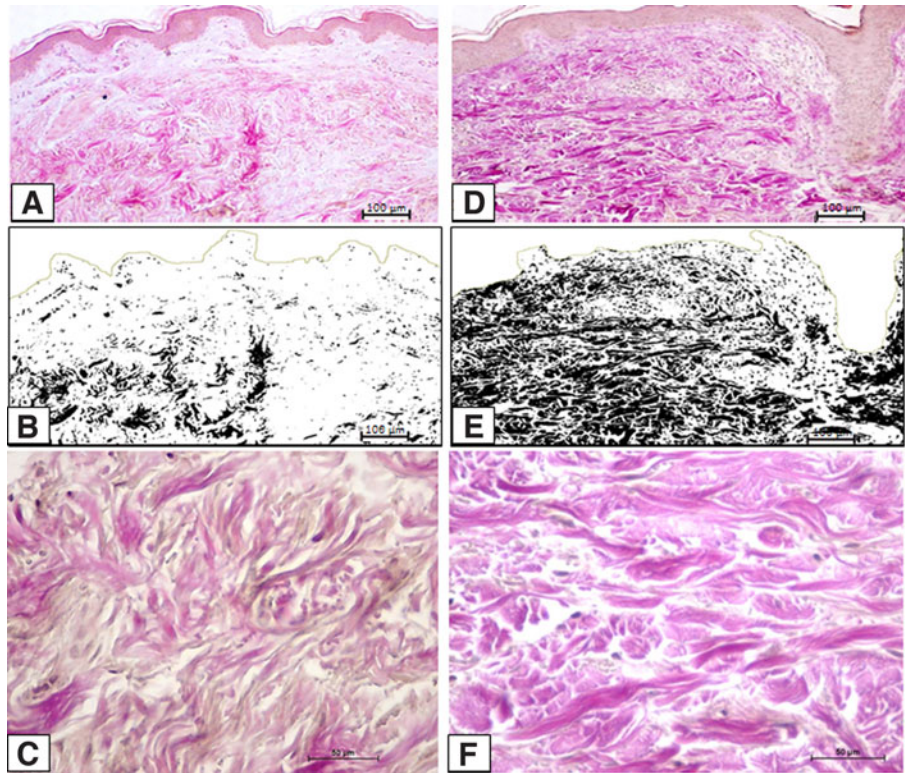
#### **Results**

Histology of the treated and untreated skin biopsies showed substantial differences. Digital morphometric analysis was performed. Connective tissue fibers present in the dermis were assessed after removing the epidermis using the freehand mode to estimate the percentage of fibers on units in the areas with connective tissue alone. After the treatment, we observed a prominent increase in thin fibers; the percentage of fibers per unit area of connective tissue had tripled in the treated areas (11.4% and 42.4%, respectively, for the nontreated and treated areas; Fig. 2). The increase in collagen fibers in the post-treatment dermis resulted in increased dermal thickness. The dermal thickness was measured three times in the untreated and treated areas, and the mean and standard deviation were calculated. Dermal thickness of the untreated area was  $1453 \pm 86$  versus  $1740 \pm 54 \mu$ m in the treated ones. No inflammatory reactions or changes were noted in the epidermis after H&E staining (Fig. 3). Picrosirius red staining with its enhancement of collagen birefringence helped in the identification and differentiation of big bundles of collagen (mature) from the smaller fibers and fibrils (newly formed) through a scale of colors by circularly polarized microscopy. The result of the treatment showed a significant increase of thin and newly formed fibers in the treated areas (Fig. 4). In the treated sample (Fig. 4D), the collagen constituted of fibers that had a predominantly yellow-green color upon observation,

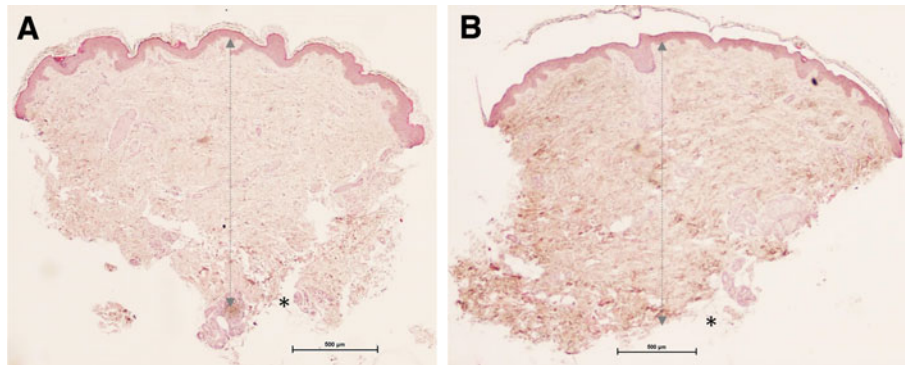


**FIG. 1.** Photos of the treated area (A before removal, B after removal).

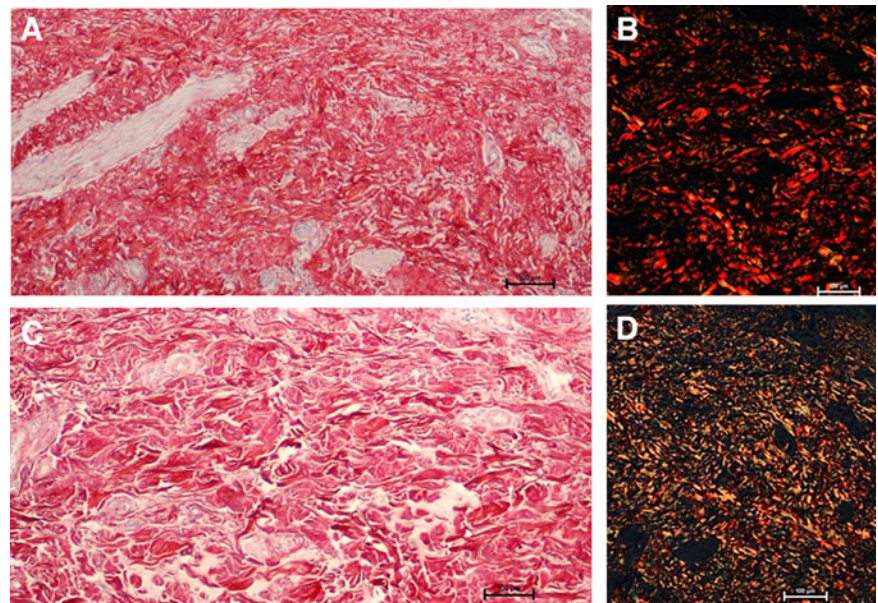
**FIG. 2.** Histology of skin biopsy of untreated (A–C) and treated (D–F) areas. Image B and E were obtained by binary segmentation (ImageJ; NIH) of originals image A and D. The reticular layer (deep dermis) shows a lower compactness of the collagen fibers after treatment; there are no collagen fiber bundles, but thinner fibers, more parallel and straighter (Van Gieson staining). (A, B, D, and E scale bars  $\times 10$ ; C and F scale bars  $\times 40$ ).



**FIG. 3.** Histology of skin biopsy of untreated (A) and treated (B) areas; tissue samples were stained with H&E. Dermal thickness was also greater in treated areas. The asterisk indicates the presence of fat cells and so the measuring point from the epidermis; in fact, fat cells indicate the limit between reticular dermal layer and hypodermis (A and B scale bars  $\times 4$ ). H&E, hematoxylin and eosin.



**FIG. 4.** Picrosirius red-stained sections of untreated (A, B) and treated (C, D) areas. Untreated (A) connective tissue of reticular dermis is intensely stained (bundles fibers). After treatment (C), connective tissue is mainly formed by thin fibrils. Part of the same sections, observed at the circularly polarized light microscope, are represented in (B) and (D), respectively. The visible colored structures are constituted by collagen fibers, which, without any additional filter, are showing different colors, appearing red, or orange (B), or green or yellow (D). This is due to different collagens and specific interactions with the Picrosirius red stain (A–D scale bars  $\times 10$ ).



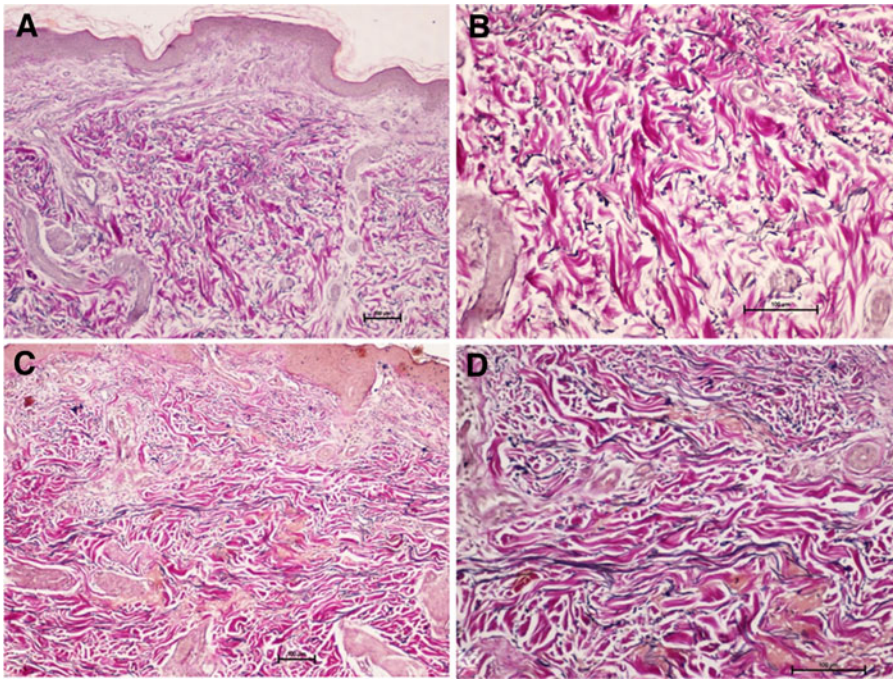


**FIG. 5.** Histology of skin biopsy of untreated (**A, B**) and treated (**C, D**) areas based on Weigert Van Gieson staining. Treated areas show that the elastic fibers (dark fibers) are more parallel and straighter in the dermis (**A** and **C** scale bars  $\times 10$ ; **B** and **D** scale bars  $\times 20$ ).

unlike the untreated sample (Fig. 4B) in which the fibers had a clear prevalence of red or red-orange color. This difference in colors represents collagen renewal, that is, post-treatment fibers mainly comprise newly synthesized collagen.

The skin specimen collected from the treated area showed more parallel and straighter reticular elastic fibers in the dermis (Fig. 5). In addition, small aggregates of existing elastin, resulting from the oxidation processes (aging, stress, etc.), were only seen in the untreated skin sample. This contrasted with that after treatment, in which elastic fibers were compact and clearly visible as longitudinally extended bundles.

## Discussion

In this case report, we assessed the changes in collagen and elastin fibers of the treated skin, without concomitant skewing of the inflammatory infiltrate. This case may serve as proof of concept for larger studies on the potential benefits of RedTouch laser for the treatment of aging skin.

In comparison to the systems currently in use, which target water to treat scars or skin aging, the RedTouch system acts directly on the dermal collagen component. The wavelengths between 650 and 950 nm can reach the deeper structures of the skin as it is weakly absorbed by water, hemoglobin, collagen, and proteins. Wavelengths below 650 nm are highly absorbed by hemoglobin and the ones over 950 nm are mainly absorbed by water. The 675-nm laser system that we used selectively targets dermal collagen.<sup>1,2</sup> The depth reached during each emission by the device is 400  $\mu\text{m}$ . Laser energy conducts heat to the dermis causing immediate collagen shrinkage and denaturation with new collagen formation and consequent wrinkle “smoothing,”<sup>3</sup> as was observed by the increase in collagen fibers in this case report. The laser created 1-mm wide thermal zones with no damage to the epidermis that was avoided due to the contact cooling system. No formation of microscopic epidermal necrotic debris or dermo-epidermal detachment was observed.

This is a considerable advantage compared to the healing time of fractional laser procedures that use a near-infrared emission with a smaller spot size (100–300  $\mu\text{m}$ ).<sup>2,3</sup> The absence of crusts and/or microcrusts makes post-treatment management and quality of life better for the patient. Procedure-related pain was minimal due to preliminary skin cooling and compression that induced transient ischemia in the treated areas.<sup>1–3</sup> The RedTouch laser may be implicated in thermal modulation of the elastic component of the dermis. This is because polypentapeptides from elastin demonstrate a temperature-dependent transition from a poor to a well-organized state.<sup>11–15</sup>

## Conclusions

The clinical and histological outcomes seen in this case report showed a substantial increase in thin and newly formed collagen fibers, resulting in greater dermal thickness. These results seem to confirm the effectiveness of this new laser technique on a cellular level. Further studies with larger cohorts will be necessary to confirm the findings of this case report.

## Author Disclosure Statement

No competing financial interests exist.

## Funding Information

There was no funding received for this study.

## References

1. Cannarozzo G, Silvestri M, Tamburi F, et al. A New 675-nm Laser Device in the treatment of acne scars: an observational study. *Lasers Med Sci* 2021;36:227–231.
2. Nisticò SP, Tolone M, Zingoni T, et al. A new 675 nm Laser Device in the treatment of melasma: results of a prospective observational study. *Photomedicine, Photobiomodulation and laser Surgery. Photobiomodul Photomed Laser Surg* 2020;38:560–564.

3. Cannarozzo G, Fazia G, Bennardo L, et al. A new 675 nm Laser Device in the treatment of facial aging: a prospective observational study. *Photomedicine, Photobiomodulation Laser Surg* 2021;39:118–122.
4. Scholkmann F, Kleiser S, Metz AJ, et al. A review on continuous wave functional near-infrared spectroscopy and imaging instrumentation and methodology. *Neuroimage* 2014;85 Pt 1:6–27.
5. Nistico SP, Del Duca E, Tamburi F, et al. Superiority of a vitamin B12-barrier cream compared with standard glycerol-petrolatum-based emollient cream in the treatment of atopic dermatitis: a randomized, left-to-right comparative trial. *Dermatol Ther* 2017;30:e12523.
6. Fullmer HM, Lillie RD. The staining of collagen with elastic tissue stains. *J Histochem Cytochem* 1957;1:11–14.
7. Putschler H, Waldrop FS, Valentine LS. Polarization microscopic studies of connective tissue stained with picrosirius red FBA. *Beith Path* 1973;150:174–187.
8. Junqueira LC, Bignolas G, Brentani RR. Picrosirius staining plus polarization microscopy, a specific method for collagen detection in tissue sections. *Histochem J* 1979;11: 447–455.
9. Frohlich MW. Birefringent objects visualized by circular polarization microscopy. *Stain Technol* 1986;61:139–143.
10. Junqueira LCU, Cossermelli W, Brentani R. Differential staining of collagens type I, II and III by sirius red and polarization microscopy. *Arch Histol Jap* 1978;41:267–274.
11. Reiersen H, Clarke AR, Rees AR. Short elastin-like peptides exhibit the same temperature-induced structural transitions as elastin polymers: implications for protein engineering. *J Mol Biol* 1998;283:255–264
12. Urry DW. Entropic elastic processes in protein mechanisms. II. Simple (passive) and coupled (active) development of elastic forces. *J Protein Chem* 1988;7:81–114.
13. Urry DW, Luan CH, Peng SQ. Molecular biophysics of elastin structure, function and pathology. *Ciba Found Symp* 1995;192:4–22
14. Li B, Alonso DO, Daggett V. The Molecular basis for the inverse temperature transition of elastin. *J Mol Biol* 2001; 305:581–592.
15. Li B, Daggett V. The molecular basis of the temperature- and pH-induced conformational transitions in elastin-based peptides. *Biopolymers* 2003;68:121–129.

Address correspondence to:

*Luigi Bennardo, MD*

*Unit of Dermatology*

*Dipartimento di Scienze Della Salute*

*Università Magna Graecia di Catanzaro*

*Catanzaro 88100*

*Italy*

*E-mail: luigibennardo10@gmail.com*

Received: July 19, 2020.

Accepted after revision: December 28, 2020.

Published online: May 26, 2021.